Supplemental Material

Mediator dynamics during heat shock in budding yeast

Debasish Sarkar[1], Z. Iris Zhu[3], Elizabeth R. Knoll[1,2], Emily Paul[2#], David Landsman[3], and Randall H. Morse[1,2*]

Supplemental items

Supplemental methods

Supplemental Fig S1. Pol II recruitment following heat shock.

Supplemental Fig S2. Effect of heat shock on Mediator association.

Supplemental Fig S3. Browser scans showing Med15 occupancy in *kin28AA* yeast and the parent strain, both treated with rapamycin, with and without heat shock.

Supplemental Fig S4. Comparison of Mediator occupancy in wild type yeast and after Kin28 depletion, with and without heat shock.

Supplemental Fig S5. Pol II and Mediator occupancy at subsets of RP genes.

Supplemental Fig S6. Mediator association at high and low Hmo1-binding UAS genes repressed by heat shock in wild type and *hmo1Δ* yeast.

Supplemental Fig S7. Mediator and Pol II occupancy at non-RP, Rap1-binding genes before and after heat shock.

Supplemental Fig S8. Persistent Mediator occupancy at non-RP genes.

Supplemental Fig S9. Effect of depleting PIC components on Mediator association with gene promoters.

Supplemental Fig S10. Effect of depleting PIC components on Mediator association with gene promoters of TATA-containing and TATA-less promoters, and Hsf1 targets divided into SAGA-dominated and TFIID-dominated promoters.

Supplemental Fig S11. Mediator association subsets of RP genes after $CdCl_2$ exposure.

Supplemental Fig S12. Browser scans showing Rap1 and Hmo1 occupancy in wild type yeast and Med15 occupancy in *kin28AA* yeast at representative Rap1-binding RP genes.

Supplemental Fig S13. Effect on Pol II and Mediator occupancy of $CdCl_2$ exposure at UAS genes.

Supplemental Fig S14. Cartoon of Mediator recruitment and transcriptional activation.

Supplemental Fig S15. Spearman correlation coefficients for 15 ChIP-seq experiments examining occupancy of Med15.

Supplemental Table S1. Ratios of Med15 occupancy in *kin28-AA* yeast compared to the parent strain YFR1321 without and with heat shock and in the presence of rapamycin.

Supplemental Table S2. Gene sets used in this study.

Supplemental Table S3. Genes from top 500 occupied by Pol II (no heat shock) down-regulated >4x by heat shock.

Supplemental Table S4. Analysis of promoters from the 1000 showing highest Pol II occupancy, and increased occupancy >3X (371 genes) , after CdCl2 exposure.

Supplemental Table S5. Yeast strains used in this study.

Supplemental Table S6. Summary of ChIP-seq experiments.

Supplemental Methods

Yeast strains and growth

Epitope tags were introduced into BY4741 to generate strains TBY100 and RMYDS2, and into YFR1321 to generate RMYDS10, by PCR amplification from strains containing the tagged protein and selectable marker, followed by transformation and selection (Hill et al. 1991; Longtine et al. 1998); strains were verified by PCR and ChIP. Cultures were grown in yeast peptone dextrose (YPD) medium (1% bacto-yeast extract, 2% bacto-peptone extract, 2% glucose). For Rap1 ChIP in wild type and *rap1-ts* yeast (Li et al. 2011), cultures were shifted to 37˚C for 1 hr before cross-linking and ChIP and processed as described previously (Paul et al. 2015a).

ChIP-seq

ChIP was performed as described previously (Knoll et al. 2018). For IP, 600 µL of whole cell extract (WCE) prepared from a 50 ml culture was incubated overnight at 4°C with 10µg of monoclonal RNA Poll antibody (Biolegend, USA), 2µg of anti-myc antibody (Sigma), or 2 µg of anti-Rap1 antibody (Santa Cruz, USA). Sixty microliters of WCE was used as Input control. Immunoprecipitated DNA was purified using 40 µL of protein A or G beads (Amersham/GE) with gentle agitation at 4°C for 90 min, and cleanup and purification performed as described previously (Knoll et al. 2018).

Libraries were prepared for sequencing using the NEBNext Ultra II library preparation kit (New England Biolabs, USA) according to manufacturer's protocol and barcoded using NEXTflex barcodes (BIOO Scientific, Austin, TX, USA) or NEBNext Multiplex Oligos for Illumina. Purification and the size selection step were performed on barcoded libraries by isolating fragment sizes between 200 and 500 bp by using AMPureXP beads (Beckman Coulter, USA); size selection was confirmed by Bioanalyzer. Sequencing was performed at the Illumina NextSeq platform at the Wadsworth Center, New York State Department of Health (Albany, NY, USA) or, for Rap1 ChIP-seq, at the Carolina Center for the Genome Sciences, University of North Carolina at Chapel Hill. Data from biological replicate experiments were analyzed separately with the exception of Figure 4C and Supplemental Figure S6, in which, because of low signal to noise in individual experiments, data was combined from four replicates for Med15 occupancy in wild type yeast (BY4741) and three replicates for *hmo1*Δ yeast. Correlation analysis (determined using the Galaxy server) of ChIP-seq experiments examining Med15 occupancy supports good reproducibility between replicates (Supplemental Figure S15).

ChIP-seq analysis

Unfiltered sequencing reads were aligned to the *S. cerevisiae* reference genome (Saccer3) using bwa (Seoighe and Wolfe 1999). Up to 1 mismatch was allowed for each aligned read. Reads mapping to multiple sites were retained to allow evaluation of associations with non-unique sequences (Seoighe and Wolfe 1999). Calculation of coverage, as shown in heat maps and line graphs, was preceded by library size normalization, and was performed with the "chipseq" and "GenomicRanges" packages in BioConductor (Gentleman et al. 2004). Alternatively, reads were aligned and analysis conducted using the Galaxy platform (Goecks et al. 2010) and Excel. For metagene analysis, including heat maps, we subtracted reads from an input control (strain YFR1321, the parent strain to *kin28*-AA yeast (KHW127), grown in the absence of rapamycin); use of a different input control (Knoll et al. 2018) yielded indistinguishable results. For Rap1, reads from the *rap1-2 ts* mutant, which has greatly reduced binding at 37˚C (Drazinic et al. 1996; Ganapathi et al. 2011), were subtracted from the wild type strain also grown at 37˚C for one hour. For line graphs, baselines were rescaled to adjust for different background levels. Heat maps and line graphs shown in the figures were from representative experiments with replicates shown as supplemental figures in most cases. Experiments comparing *hmo1*Δ and BY4741 yeast (Figure 4C and Supplemental Figure S6B-C) yielded low signal; for these experiments, data from three BY4741 replicates and four *hmo1*Δ replicates were combined to produce the resulting line graphs and heat maps.

Pol II occupancy was determined as read depth over ORFs, normalized for length, and Mediator occupancy was determined as normalized read depth over the 300 bp upstream of TSS

using BedCov in SamTools (Li et al. 2009). Clustering analysis (Supplemental Fig. S1) was performed using Cluster and Treeview (Eisen et al. 1998). The 1000 genes having highest Pol II occupancy were obtained using BedCov from SamTools to obtain read depth over coding sequences using Pol II ChIP-seq data (strain BY4741 grown at 30˚C in YPD medium) (Paul et al. 2015b; Knoll et al. 2018). Genes designated as SAGA-dominated and TFIID-dominated were obtained from (Huisinga and Pugh 2004), and genes designated as containing or not containing a consensus TATA element, and being Taf1-enriched or Taf1-depleted, were obtained from (Rhee and Pugh 2012). Targets of Hsf1 were defined as those genes that are not activated by heat shock if Hsf1 is depleted (Pincus et al. 2018; Tye et al. 2019), Msn2/4 targets were defined in (Solis et al. 2016), and CdCl2 induced genes labeled "Momose" in the figures were those identified in Table 3 of (Momose and Iwahashi 2001). RP genes were divided into Abf1-binding genes (nine genes; we also included *RPL15B*, which is a "Category III" gene according to (Knight et al. 2014), and appears to bind Abf1 and Rap1 poorly if at all) and Rap1-binding genes that do or do not bind Hmo1 according to (Knight et al. 2014). Hmo1 occupancies were calculated over a region of 1 kb upstream of gene ORFs using BedCov from SamTools (Li et al. 2009) applied to data from (Knight et al. 2014). The various gene sets used are listed in Table S2. Occupancy profiles were normalized for read depth and generated using the Integrative Genomics Viewer (Robinson et al. 2011). Gene Ontology analysis was performed using the Generic Gene Ontology Term Finder (https://go.princeton.edu/cgi-bin/GOTermFinder/GOTermFinder) (Boyle et al. 2004). Hypergeometric test p-values were calculated using the online calculator at http://www.alewand.de/stattab/tabdiske.htm, and p-values for distributions shown in box plots were calculated using the Wilcoxon rank sum test. Box plots depict the second and third quartiles as boxes, and the first and fourth quartiles as whiskers; median values are depicted as horizontal

lines separating second and third quartiles, and outliers are represented as points above and below the whiskers.

Previously published ChIP-seq data used in this work was accessed at the NCBI BioProject database (https://www.ncbi.nlm.nih.gov/bioproject/) under accession number PRJNA413080 (Knoll et al. 2018) and PRJNA261651 (Knight et al. 2014).

References

Boyle EI, Weng S, Gollub J, Jin H, Botstein D, Cherry JM, Sherlock G. 2004. GO::TermFinder--open source software for accessing Gene Ontology information and finding significantly enriched Gene Ontology terms associated with a list of genes. *Bioinformatics* **20**: 3710-3715.

Drazinic CM, Smerage JB, Lopez MC, Baker HV. 1996. Activation mechanism of the multifunctional transcription factor repressor-activator protein 1 (Rap1p). *Mol Cell Biol* **16**: 3187-3196.

Eisen MB, Spellman PT, Brown PO, Botstein D. 1998. Cluster analysis and display of genome-wide expression patterns. *Proc Natl Acad Sci U S A* **95**: 14863-14868.

Ganapathi M, Palumbo MJ, Ansari SA, He Q, Tsui K, Nislow C, Morse RH. 2011. Extensive role of the general regulatory factors, Abf1 and Rap1, in determining genome-wide chromatin structure in budding yeast. *Nucleic Acids Res* **39**: 2032-2044.

Gentleman RC, Carey VJ, Bates DM, Bolstad B, Dettling M, Dudoit S, Ellis B, Gautier L, Ge Y, Gentry J et al. 2004. Bioconductor: open software development for computational biology and bioinformatics. *Genome Biol* **5**: R80.

Goecks J, Nekrutenko A, Taylor J. 2010. Galaxy: a comprehensive approach for supporting accessible, reproducible, and transparent computational research in the life sciences. *Genome Biol* **11**: R86.

Hill J, Donald KA, Griffiths DE, Donald G. 1991. DMSO-enhanced whole cell yeast transformation [published erratum appears in Nucleic Acids Res 1991 Dec 11;19(23):6688]. *Nucleic Acids Res* **19**: 5791.

Huisinga KL, Pugh BF. 2004. A genome-wide housekeeping role for TFIID and a highly regulated stress-related role for SAGA in Saccharomyces cerevisiae. *Mol Cell* **13**: 573-585.

Knight B, Kubik S, Ghosh B, Bruzzone MJ, Geertz M, Martin V, Denervaud N, Jacquet P, Ozkan B, Rougemont J et al. 2014. Two distinct promoter architectures centered on dynamic nucleosomes control ribosomal protein gene transcription. *Genes Dev* **28**: 1695-1709.

Knoll ER, Zhu ZI, Sarkar D, Landsman D, Morse RH. 2018. Role of the pre-initiation complex in Mediator recruitment and dynamics. *Elife* **7**.

Li H, Handsaker B, Wysoker A, Fennell T, Ruan J, Homer N, Marth G, Abecasis G, Durbin R, Genome Project Data Processing S. 2009. The Sequence Alignment/Map format and SAMtools. *Bioinformatics* **25**: 2078-2079.

Li Z, Vizeacoumar FJ, Bahr S, Li J, Warringer J, Vizeacoumar FS, Min R, Vandersluis B, Bellay J, Devit M et al. 2011. Systematic exploration of essential yeast gene function with temperature-sensitive mutants. *Nat Biotechnol* **29**: 361-367.

Longtine MS, McKenzie A, 3rd, Demarini DJ, Shah NG, Wach A, Brachat A, Philippsen P, Pringle JR. 1998. Additional modules for versatile and economical PCR-based gene deletion and modification in Saccharomyces cerevisiae. *Yeast* **14**: 953-961.

Momose Y, Iwahashi H. 2001. Bioassay of cadmium using a DNA microarray: genome-wide expression patterns of Saccharomyces cerevisiae response to cadmium. *Environ Toxicol Chem* **20**: 2353-2360.

Paul E, Tirosh I, Lai W, Buck MJ, Palumbo MJ, Morse RH. 2015a. Chromatin mediation of a transcriptional memory effect in yeast. *G3 (Bethesda)* **5**: 829-838.

Paul E, Zhu ZI, Landsman D, Morse RH. 2015b. Genome-wide association of mediator and RNA polymerase II in wild-type and mediator mutant yeast. *Mol Cell Biol* **35**: 331-342.

Pincus D, Anandhakumar J, Thiru P, Guertin MJ, Erkine AM, Gross DS. 2018. Genetic and epigenetic determinants establish a continuum of Hsf1 occupancy and activity across the yeast genome. *Mol Biol Cell* **29**: 3168-3182.

Rhee HS, Pugh BF. 2012. Genome-wide structure and organization of eukaryotic pre-initiation complexes. *Nature* **483**: 295-301.

Robinson JT, Thorvaldsdottir H, Winckler W, Guttman M, Lander ES, Getz G, Mesirov JP. 2011. Integrative genomics viewer. *Nat Biotechnol* **29**: 24-26.

Seoighe C, Wolfe KH. 1999. Updated map of duplicated regions in the yeast genome. *Gene* **238**: 253-261.

Solis EJ, Pandey JP, Zheng X, Jin DX, Gupta PB, Airoldi EM, Pincus D, Denic V. 2016. Defining the Essential Function of Yeast Hsf1 Reveals a Compact Transcriptional Program for Maintaining Eukaryotic Proteostasis. *Mol Cell* **63**: 60-71.

Tye BW, Commins N, Ryazanova LV, Wuhr M, Springer M, Pincus D, Churchman LS. 2019. Proteotoxicity from aberrant ribosome biogenesis compromises cell fitness. *Elife* **8**.

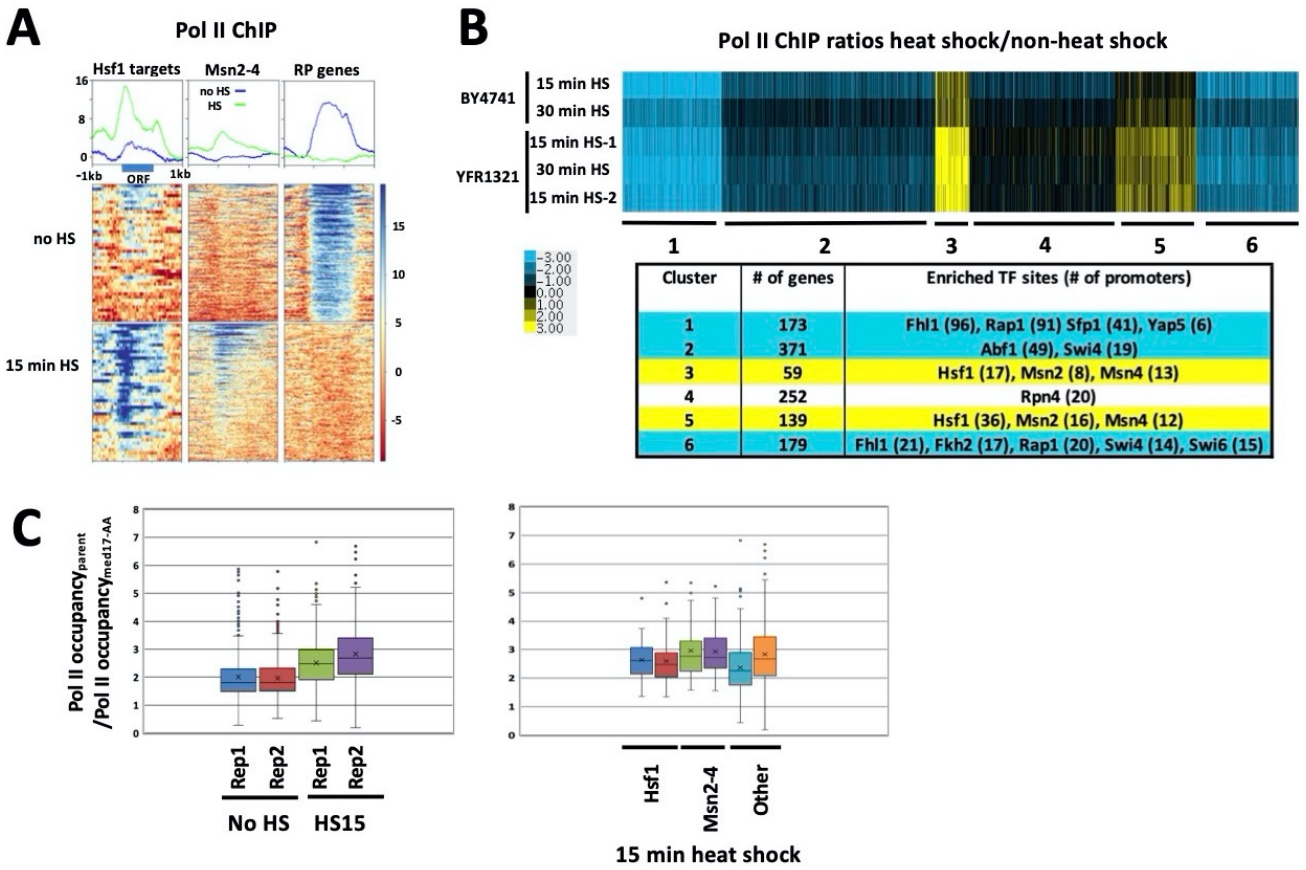

Supplemental Fig S1. Pol II recruitment following heat shock. (A) Heat maps and line graphs depicting normalized Pol II occupancy in rapamycin-treated YFR1321 cells (the parent strain for anchor-away strains) before and after 15 min heat shock at 42 Hsf1 targets and 213 Msn2-4 targets (see Methods and Supplemental Table S2) and 137 RP genes. (B) K-means clustering (K=6) was performed for the ratio of Pol II occupancy (normalized for gene length) before and after heat shock, in YFR1321 and BY4741, using the 1000 genes having highest Pol II occupancy (normalized for ORF length) under non-heat-shock conditions plus the 300 genes having highest occupancy after heat shock (1179 ORFs, due to overlap between the two sets). Enrichment for TFs in individual clusters, as shown, derived from CERES (Morris et al., 2010). (C) Effect of Med17 depletion by anchor-away on Pol II occupancy. Box and whisker plots depicting ratios of Pol II occupancy (normalized for gene length) in the parent strain, YFR1321, relative to the *med17-AA* strain (YFR1544), both treated with rapamycin, with and without heat shock, as indicated. Left panel depicts replicate experiments examining the 886 genes with highest Pol II occupancy in the absence of heat shock (three outliers with ratios >8 in replicate 1 were removed for clarity) and 294 genes having highest occupancy after heat shock. Right panel depicts the 294 genes having highest Pol II occupancy after heat shock, divided into Hsf1 targets (34 genes), Msn2-4 targets (48 genes), and other genes (212 genes).

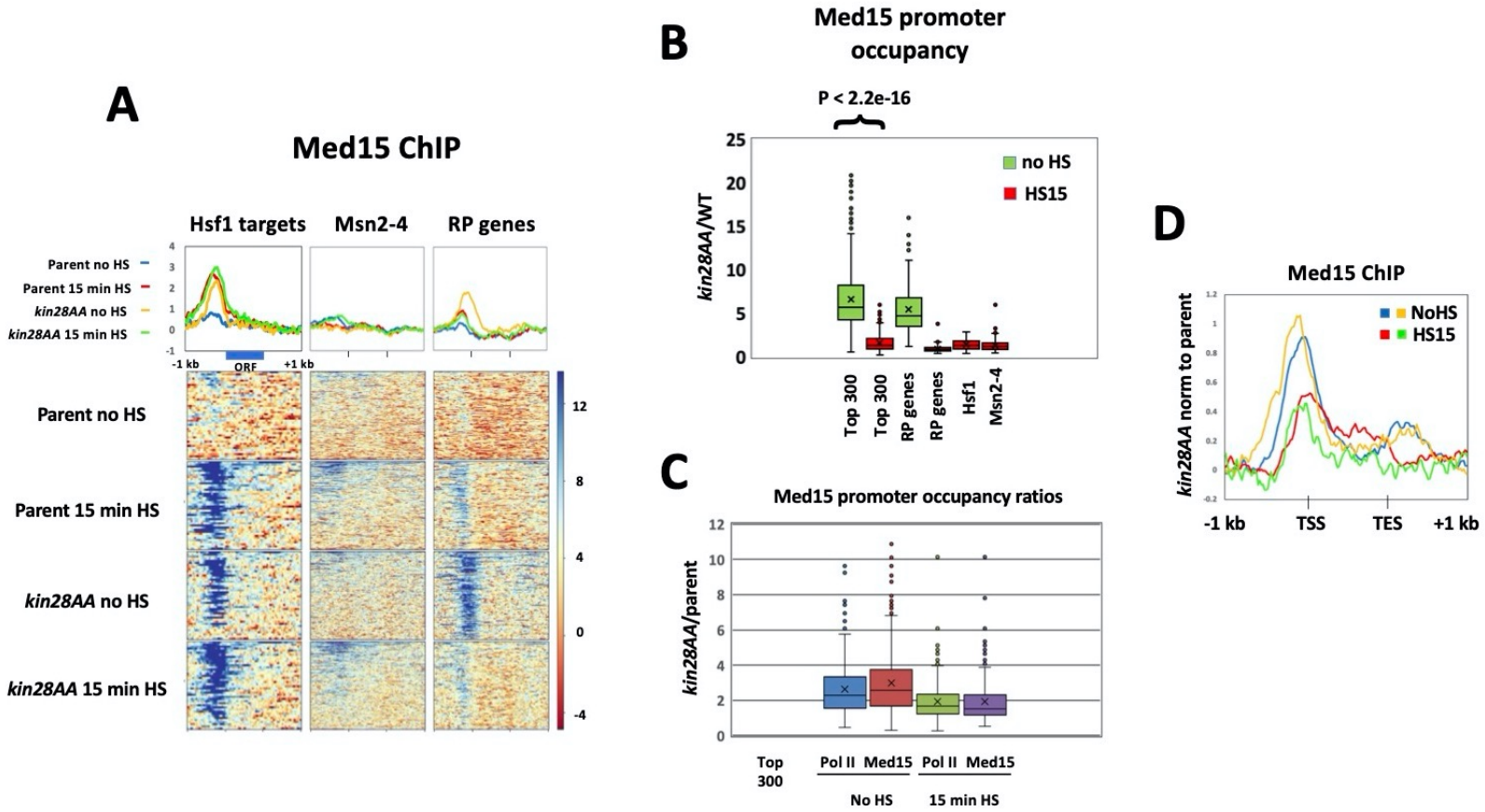

Supplemental Fig S2. Effect of heat shock on Mediator association. (A-B) Biological replicate experiment for Figure 2A. (A) Heat maps and line graphs depicting normalized occupancy of the Mediator tail module subunit, Med15, in *kin28AA* yeast treated with rapamycin and the parent strain YFR1321, also treated with rapamycin, before and after 15 min heat shock, at Hsf1 targets, Msn2-4 targets, and RP genes. (B) Box and whisker plots showing the ratios of Med15 occupancy with and without Kin28 depletion for the ~300 genes showing highest Med15 occupancy in Kin28-depleted cells without or with heat shock; ratios are also shown for RP genes, Hsf1 targets, and Msn2-4 targets in heat-shocked cells. (C) Box and whisker plots showing the ratios of Med15 occupancy with and without Kin28 depletion for the ~300 genes showing highest occupancy by Pol II or Med15, as indicated, without or with heat shock. Data same as used for Supplemental Fig S1. (D) Line graphs depicting occupancy of Med15 in *kin28-AA* yeast normalized to the parent strain, both treated with rapamycin, in each of two replicate experiments without and with heat shock. Occupancy was determined for the ~300 genes most highly occupied by Pol II after heat shock (HS15 graphs), and the 641 most highly occupied genes in the absence of heat shock (noHS graphs); the latter number was chosen based on having the same lower cutoff for occupancy as for the heat shock cohort.

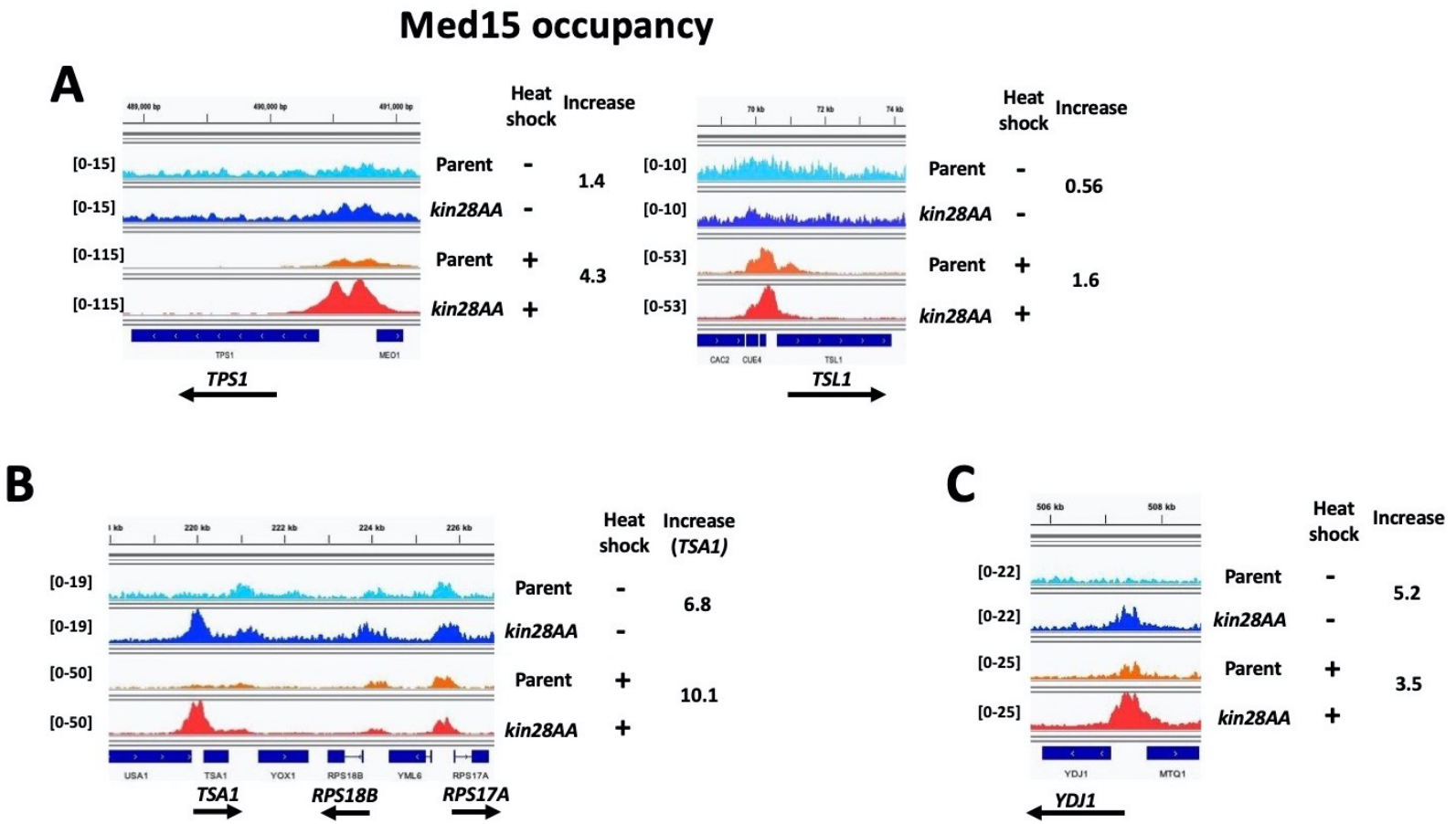

Supplemental Fig S3. Browser scans showing Med15 occupancy in *kin28AA* yeast and the parent strain, both treated with rapamycin, with and without heat shock. Scale, in reads per million mapped reads, is indicated for each scan. (A) *TPS1* and *TSL1* are Msn2/4 targets and are expressed at low levels in the absence of heat shock and induced 5-10 fold upon heat shock based on Pol II occupancy; (B) *TSA1* is expressed in the absence of heat shock and shows 2-fold increased Pol II occupancy on heat shock, and is not a target of Hsf1 or Msn2/4; and (C) *YDJ1* is a target of Hsf1 and is expressed both with and without heat shock with little change in Pol II occupancy. Note that *RPS18B* and *RPS17A* in (B) are strongly repressed upon heat shock.

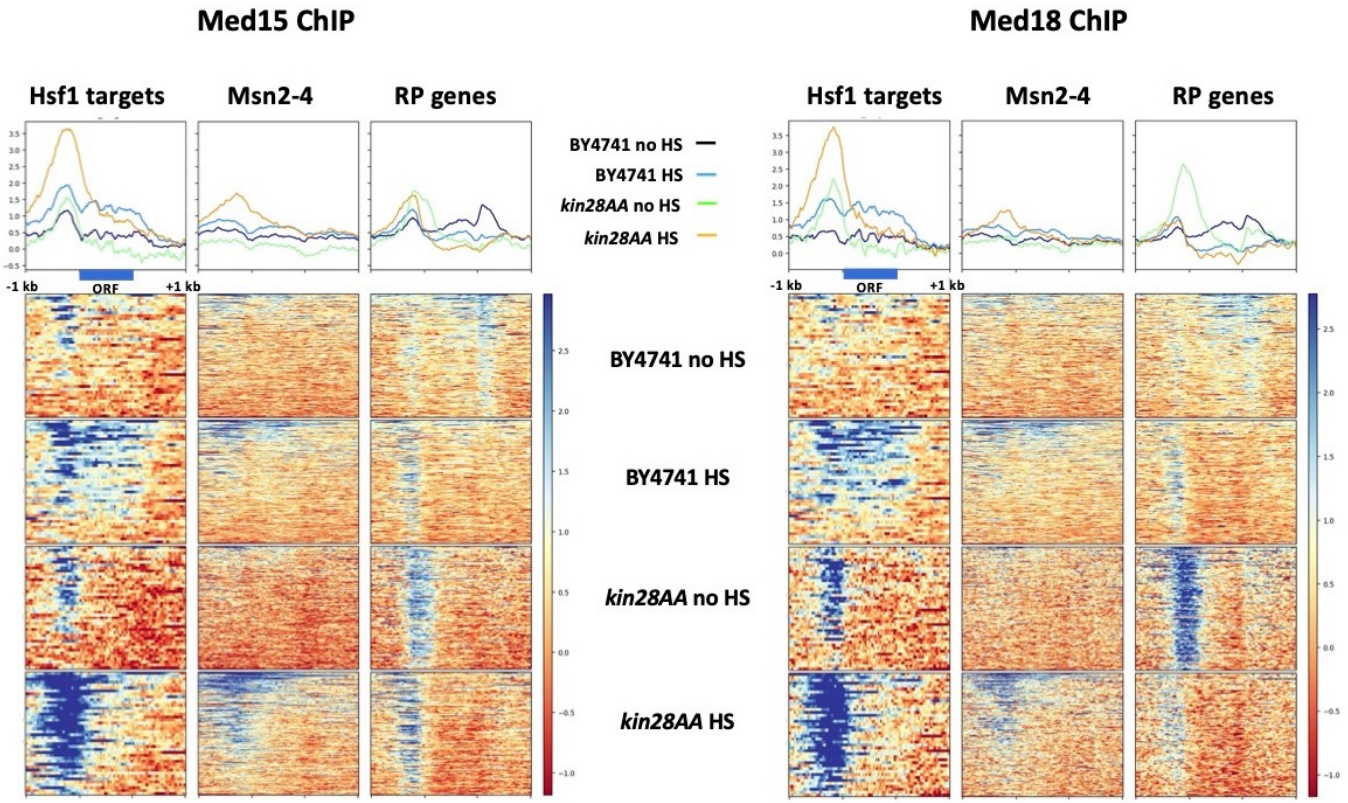

Supplemental Fig S4. Comparison of Mediator occupancy in epitope-tagged strains derived from wild type yeast (BY4741; strains TBY100 and RMYDS2) and after Kin28 depletion (*kin28AA* yeast treated with rapamycin; strains TBY128 and EKY18), with and without heat shock, at Hsf1 targets, Msn2-4 targets, and RP genes. Left, Med15 (tail module) occupancy; right, Med18 (head module) occupancy.

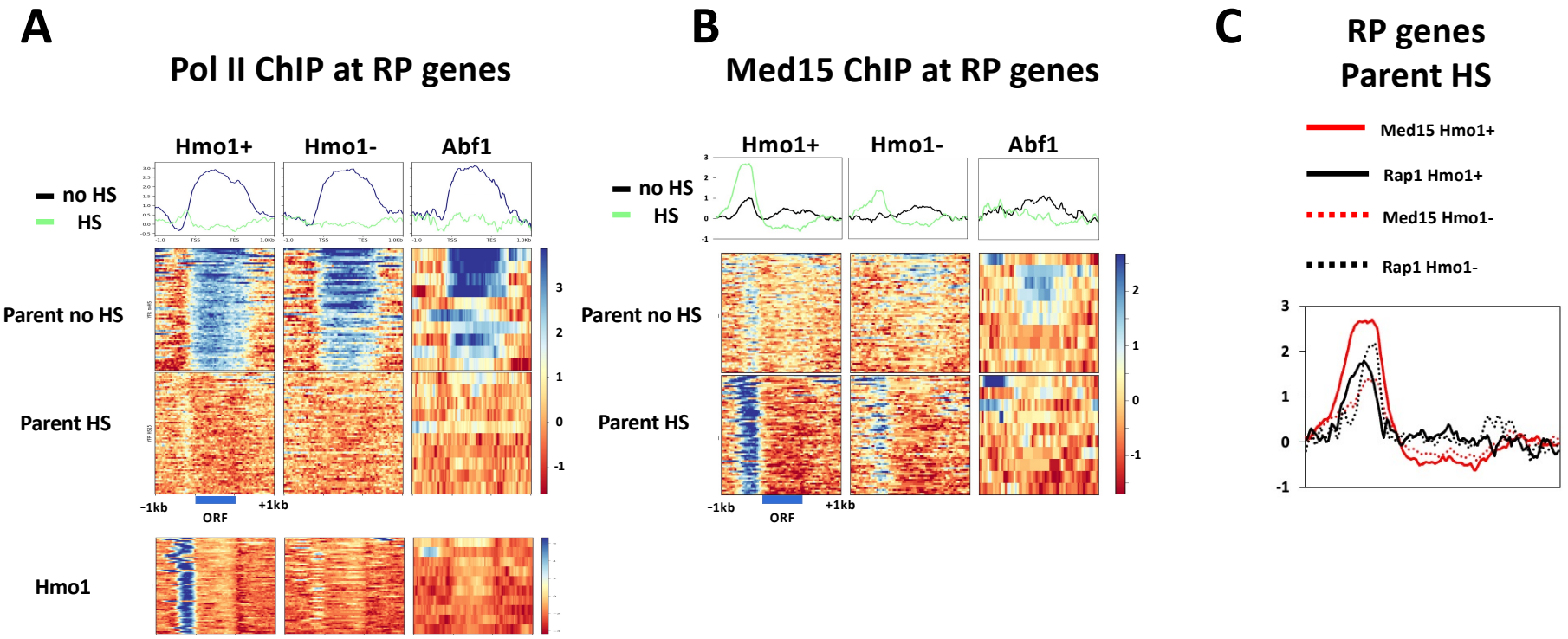

Supplemental Fig S5. Pol II and Mediator occupancy at subsets of RP genes. Heat maps and line graphs are shown for (A) Pol II and (B) Med15 (tail) in YFR1321, the parent strain for *kin28-AA* yeast, treated with rapamycin, at 69 RP genes binding Hmo1, 60 RP genes binding Rap1, Ifh1, and Fhl1 but not Hmo1, and 10 genes binding Abf1 (*RPS22B* is included in the non-Hmo1-binding gene set, according to (Knight et al., 2014), but binds Abf1 and so is also included in that set). Hmo1 binding (bottom, part (A) from ChIP-seq data from Knight et al., 2014.) (C) Line graphs depicting occupancy in YFR1321 of Med15 and Rap1 at Hmo1-binding and Hmo1-non-binding RP genes that do not bind Abf1.

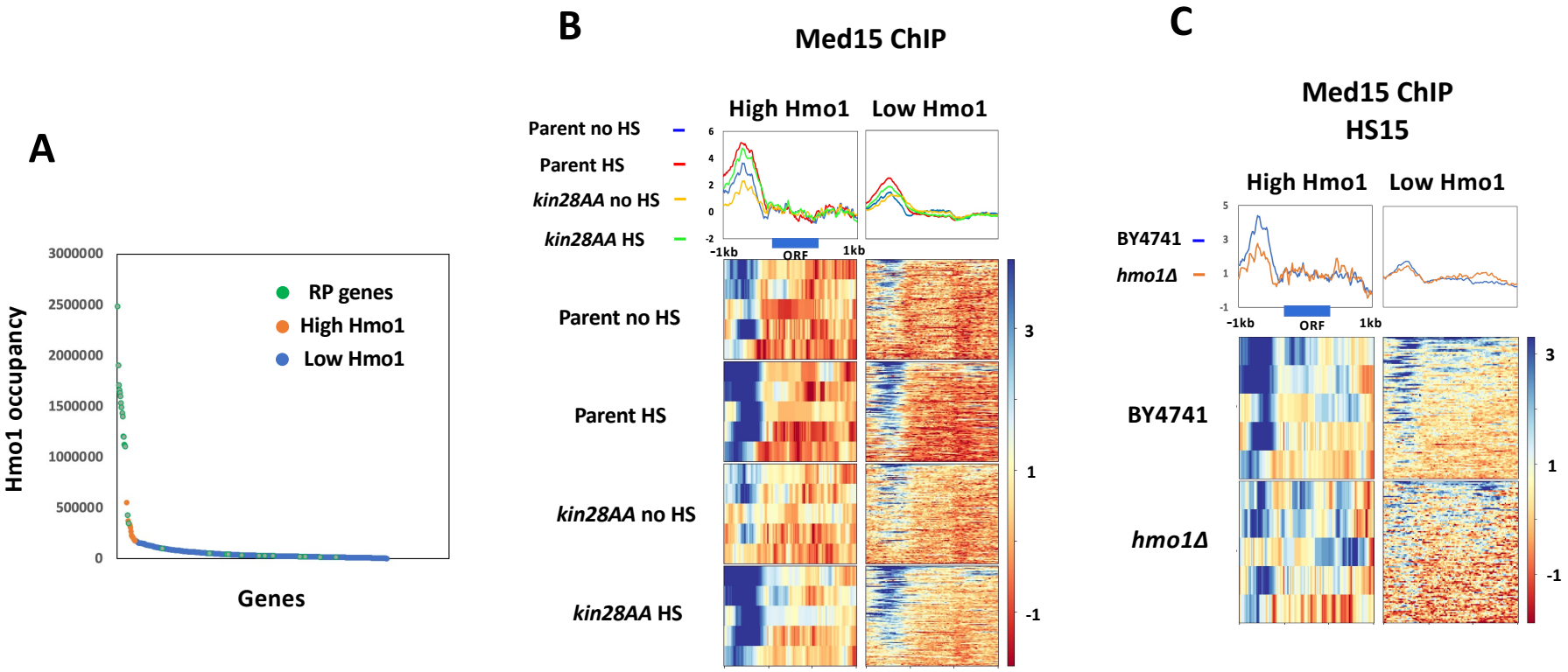

Supplemental Fig S6. Mediator association at high and low Hmo1-binding UAS genes repressed by heat shock in wild type and *hmo1Δ* yeast. (A) Hmo1 occupancy (reads summed over 1 kb upstream of ORF) at UAS genes from (Knight et al., 2014). Genes are ordered from highest to lowest Hmo1 occupancy and are designated as high and low Hmo1-binding as indicated, as are RP genes. (B) Heat maps and line graphs showing Med15 occupancy at five UAS genes down-regulated by heat shock and having high Hmo1 occupancy and at 105 down-regulated UAS genes having low Hmo1 occupancy in *kin28AA* yeast and the parent strain, both treated with rapamycin, before and after 15 min HS. (C) Heat maps and line graphs showing Med15 occupancy at five UAS genes down-regulated by heat shock and having high Hmo1 occupancy and at 105 down-regulated UAS genes having low Hmo1 occupancy in BY4741 and *hmo1Δ* yeast after 15 min HS.

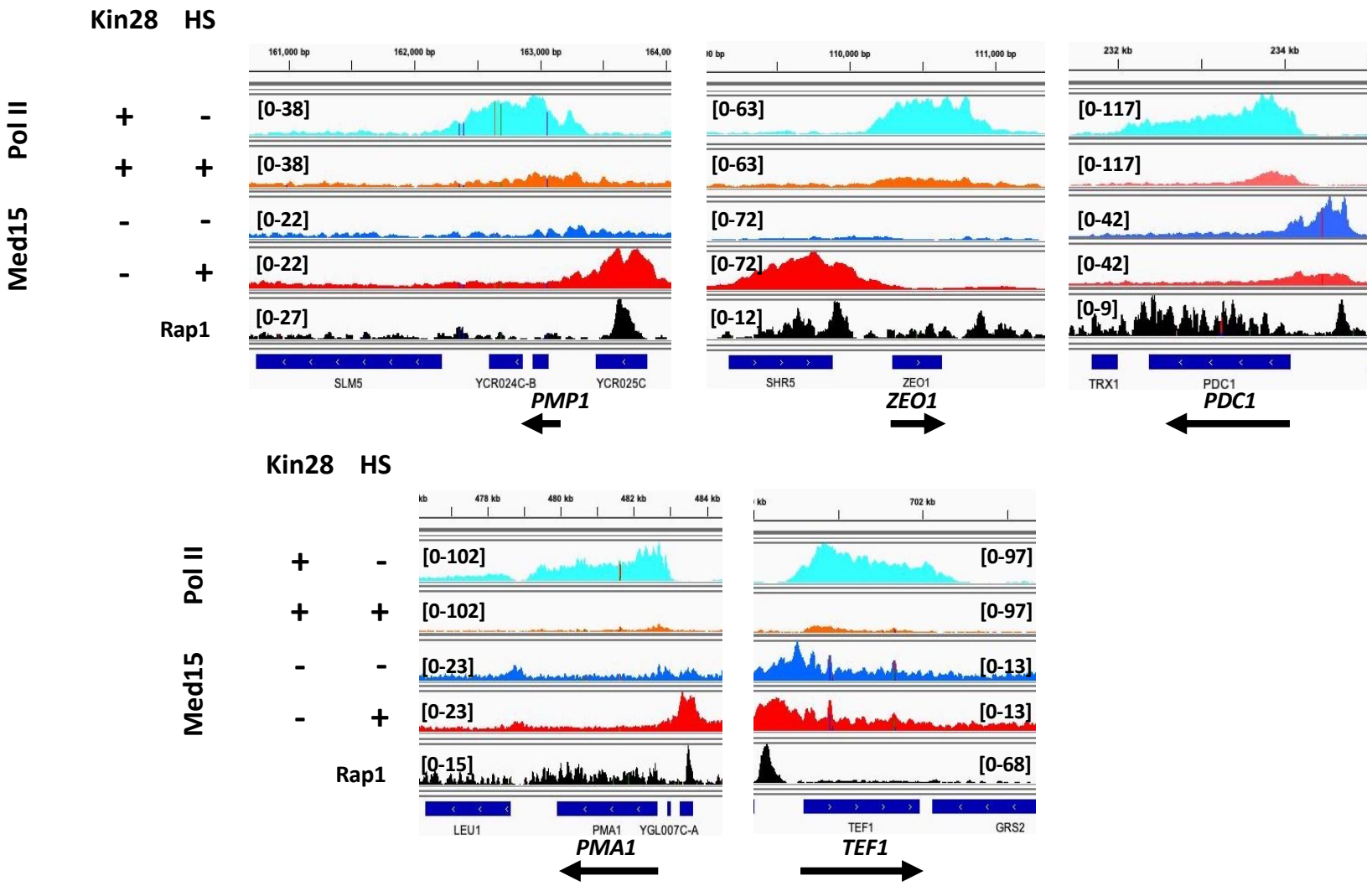

Supplemental Fig S7. Mediator and Pol II occupancy at non-RP, Rap1-binding genes before and after heat shock. Browser scans are shown for Pol II in YFR1321, the parent strain for *kin28AA* yeast, and for Med15 in *kin28AA* yeast, both treated with rapamycin; and for Rap1 in BY4741 yeast at the five non-RP, Rap1-binding genes exhibiting highest normalized Pol II occupancy in wild type, unstressed yeast. Scale, in reads per million mapped reads, is indicated for each scan.

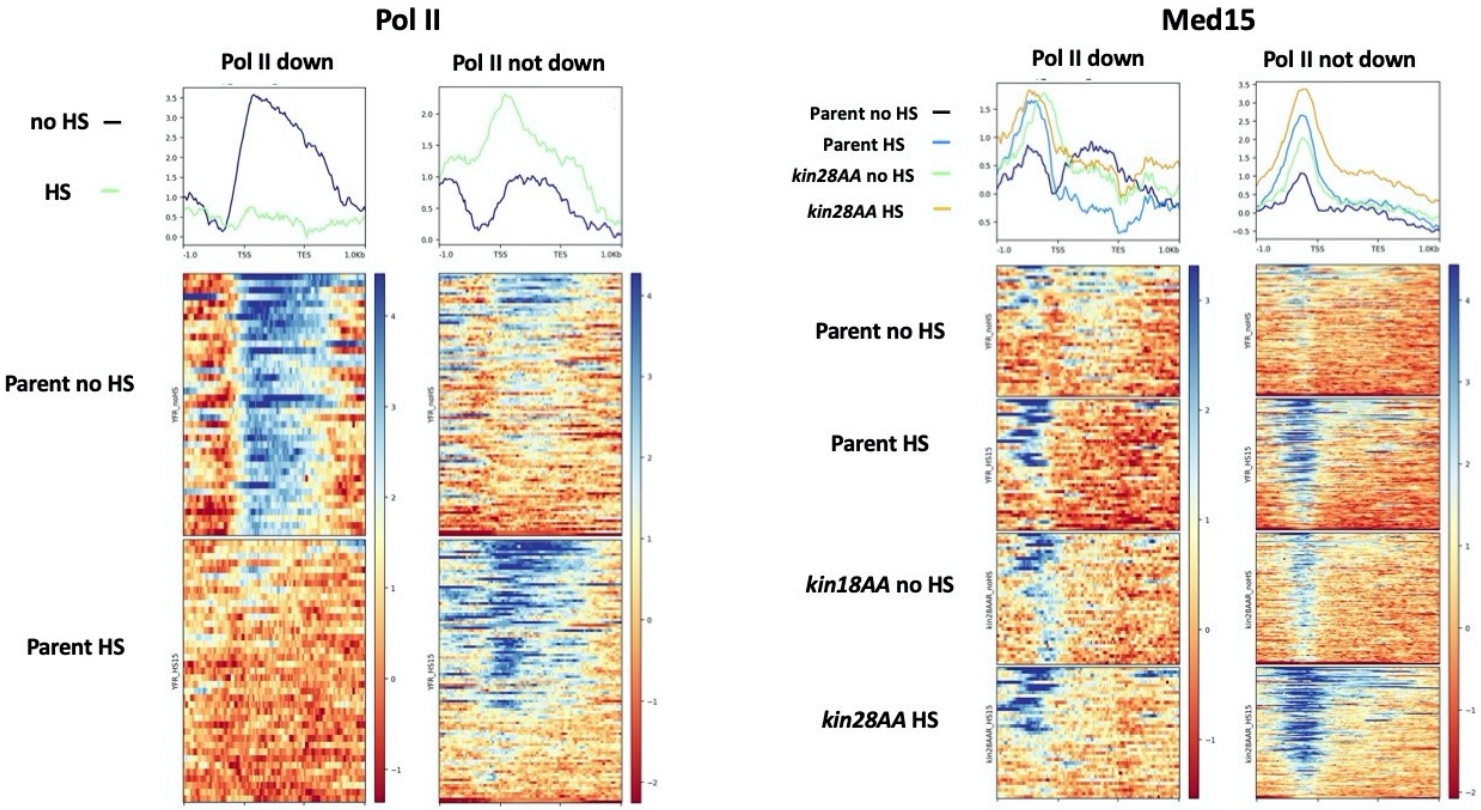

Supplemental Fig S8. Persistent Mediator occupancy at non-RP genes. Heat maps and line graphs for Pol II and Med15 (tail module) at 39 genes showing down-regulated Pol II occupancy by at least 4X ("Pol II down") upon heat shock and 97 genes showing increased or unchanged Pol II occupancy ("Pol II not down"), with both sets derived from the 500 genes exhibiting greatest Med15 occupancy in *kin28AA* yeast treated with rapamycin in the absence of heat shock. Pol II occupancy is shown in YFR1321, the parent strain for *kin28AA* yeast, and Med15 occupancy is shown for YFR1321 and *kin28AA* yeast, in both cases before and after heat shock.

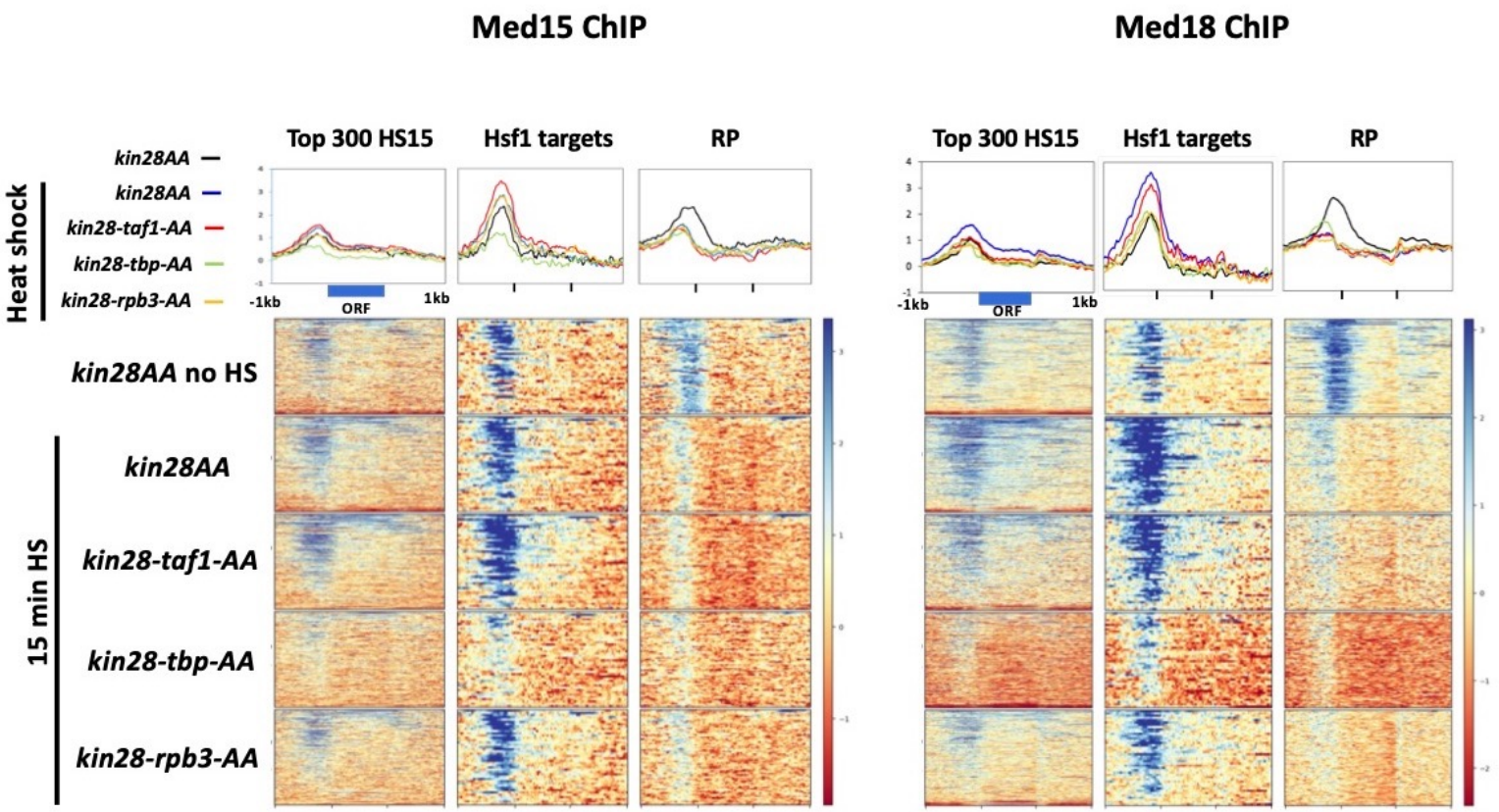

Supplemental Fig S9. Effect of depleting PIC components on Mediator association with gene promoters. Replicate experiment for Figure 5B. Heat maps and line graphs showing normalized occupancy of Med15 (tail) and Med18 (head) at the ~300 genes with highest Pol II occupancy after heat shock, Hsf1 targets, and RP genes after depletion of Kin28 alone or together with Taf1, TBP, or Rpb3, as indicated, without or with 15 min heat shock, as indicated. The Med18 ChIP sample in *kin28-tbp*-AA yeast done in parallel with the other Med18 ChIP samples in the figure failed, so a later replicate was used; this replicate differed in its baseline (note the difference in the heat map), and so the baseline for the line graph of Med18 in *kin28-tbp-AA* yeast treated with rapamycin was adjusted to conform with the other samples.

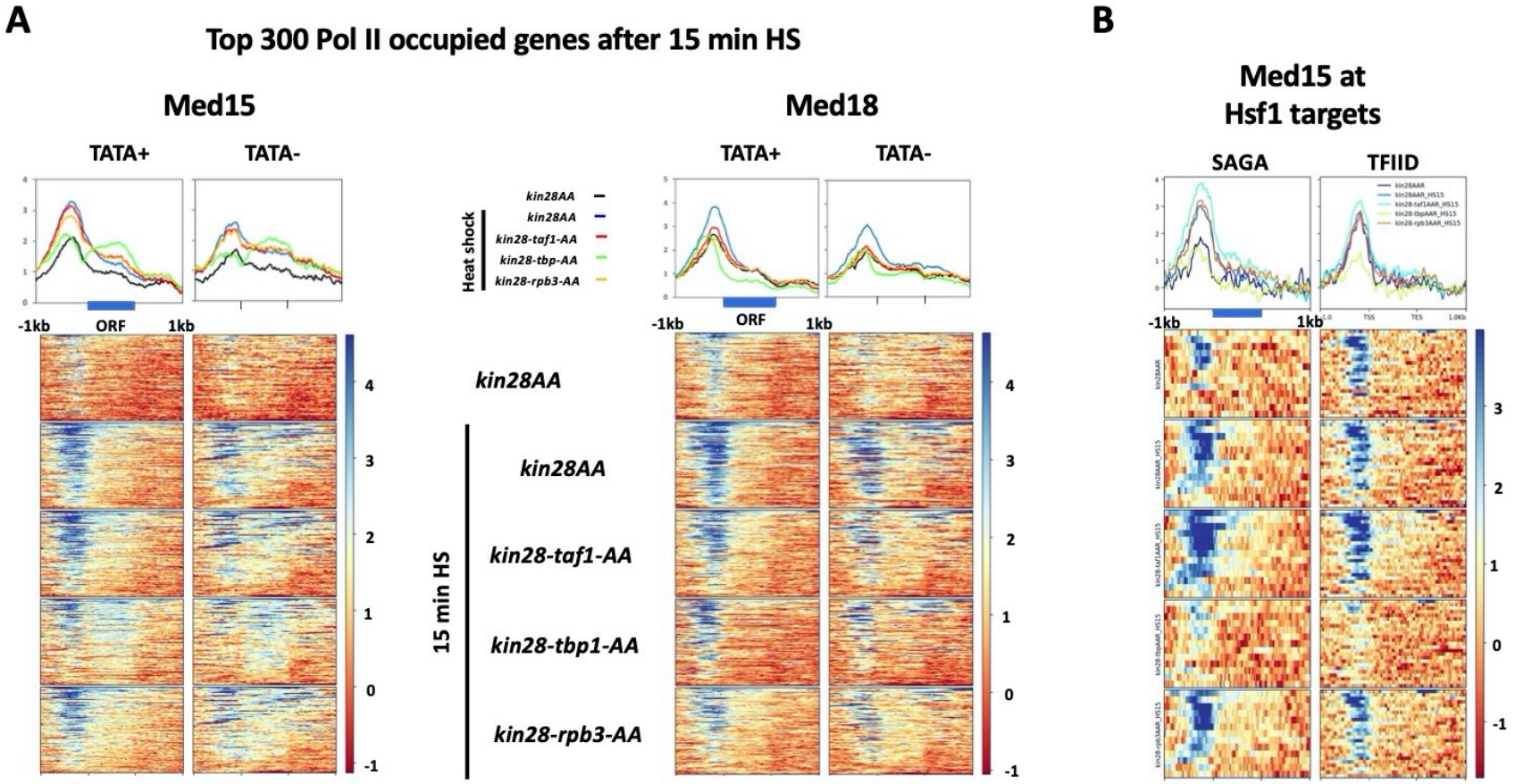

Supplemental Fig S10. Effect of depleting PIC components on Mediator association with gene promoters of (A) TATA-containing and TATA-less promoters, and (B) Hsf1 targets divided into SAGA-dominated and TFIID-dominated promoters (Table S2). (A) Heat maps and line graphs showing normalized occupancy of Med15 (tail) and Med18 (head) at TATA-containing promoters (111 genes) and TATA-less promoters (83 genes) from the 300 genes with highest Pol II occupancy after 15 min of heat shock. (B) Heat maps and line graphs for Med15 occupancy at 13 SAGA-dominated and 25 TFIID-dominated Hsf1 targets (Table S2). Occupancy is shown after depletion of Kin28 alone with or without heat shock, and after depletion of Kin28 and Taf1, TBP, or Rpb3 followed by 15 min of heat shock.

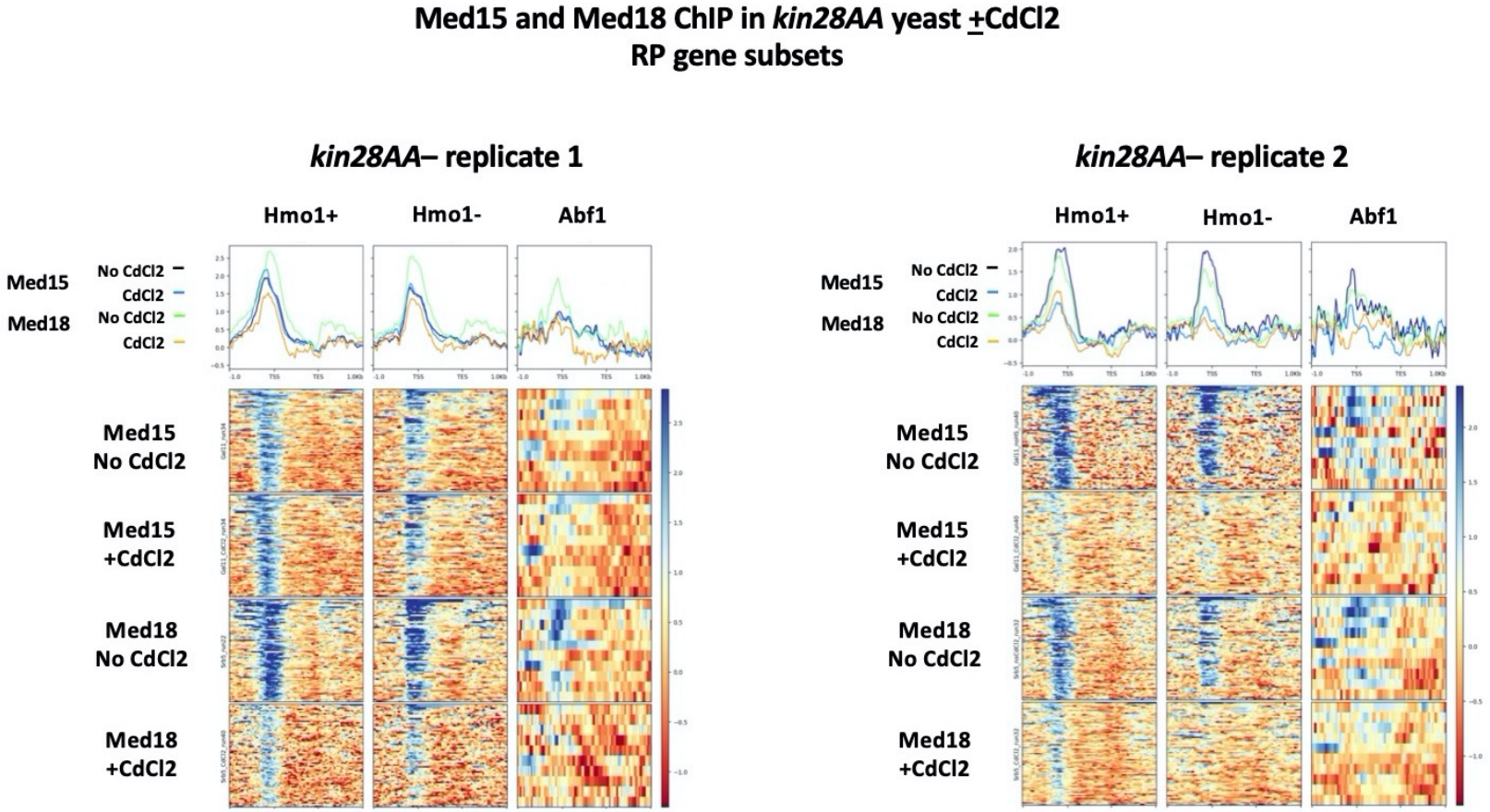

Supplemental Fig S11. Mediator association at subsets of RP genes after $CdCl_2$ exposure. Heat maps and line graphs showing normalized occupancy of Med15 and Med18 in *kin28AA* yeast treated with rapamycin, with and without $CdCl_2$ exposure, at RP genes divided into Hmo1-binding, non-Hmo1-binding, and Abf1 binding genes (Table S2).

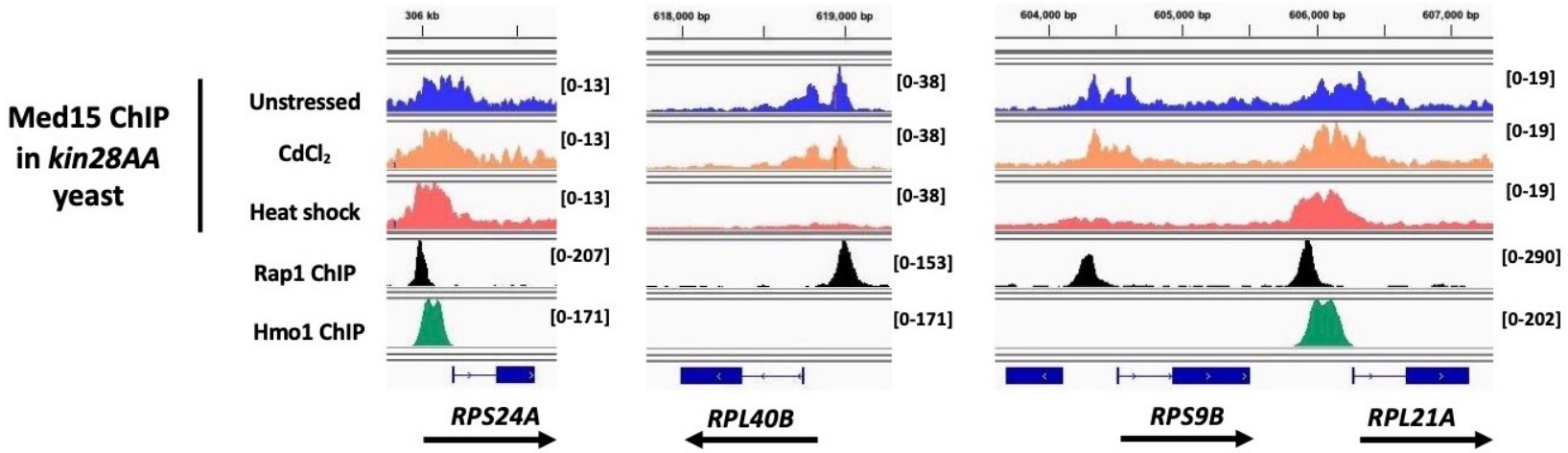

Supplemental Fig S12. Browser scans showing Med15 occupancy in *kin28AA* yeast, Rap1 occupancy in BY4741 wild type yeast, and Hmo1 occupancy in W303 wild type yeast at representative Rap1-binding RP genes. Data for unstressed and heat shock conditions, and for Rap1 and Hmo1, are the same as Figure 4. Scale, in reads per million mapped reads, is indicated for each scan.

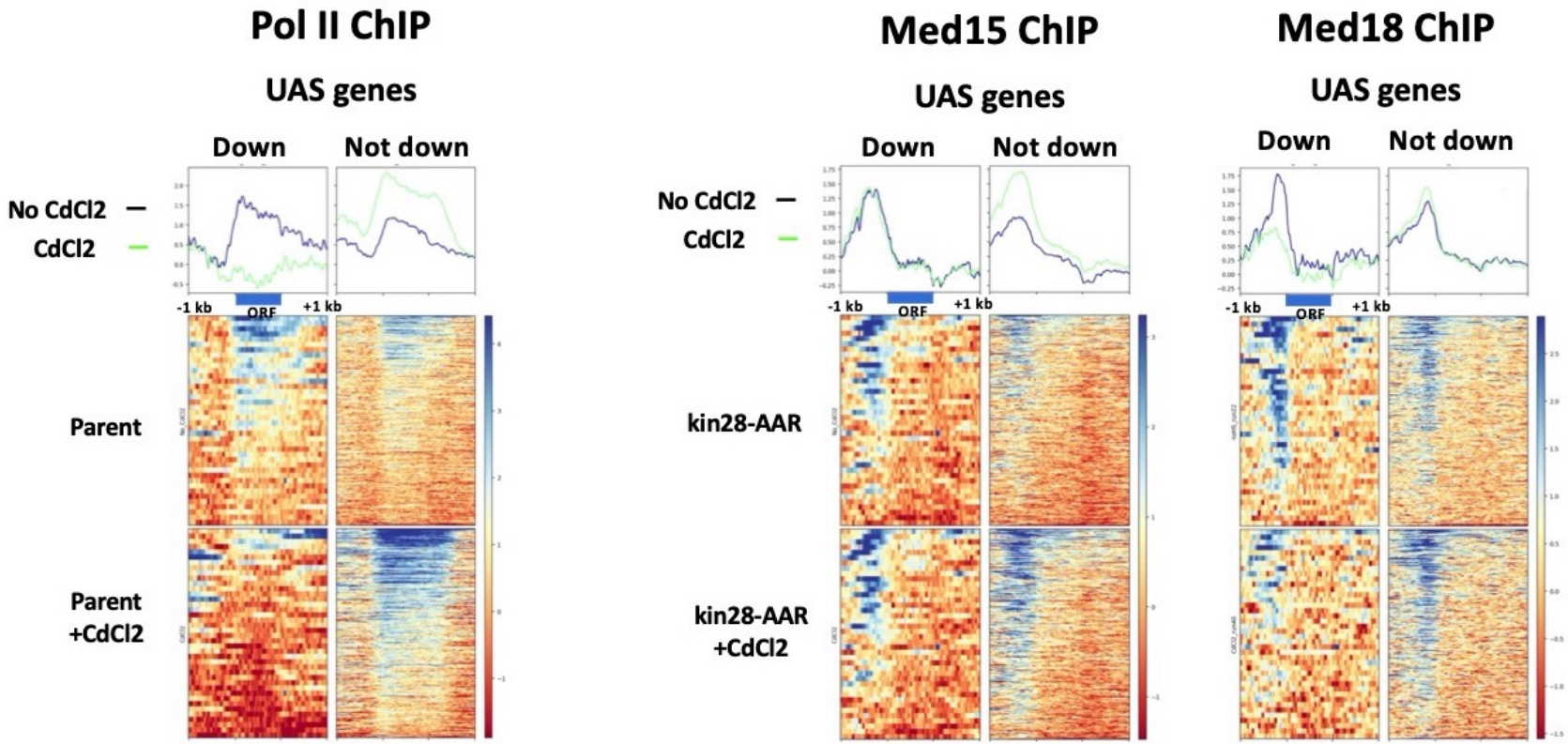

Supplemental Fig S13. Effect on Pol II and Mediator occupancy of $CdCl_2$ exposure at UAS genes. Heat maps and line graphs showing normalized occupancy of Pol II at UAS genes, separated into genes showing Pol II occupancy reduced by at least 2-fold upon $CdCl_2$ exposure and excluding RP genes ("Down", 40 genes) or having Pol II occupancy between 80% and 125% seen in untreated cells ("Not down", 286 genes). Pol II occupancy was determined in the anchor away parent strain YFR1321 with or without $CdCl_2$ exposure, and Med15 (tail module) and Med18 (head module) occupancies were measured in *kin28-AA* yeast treated with rapamycin with or without $CdCl_2$ exposure.

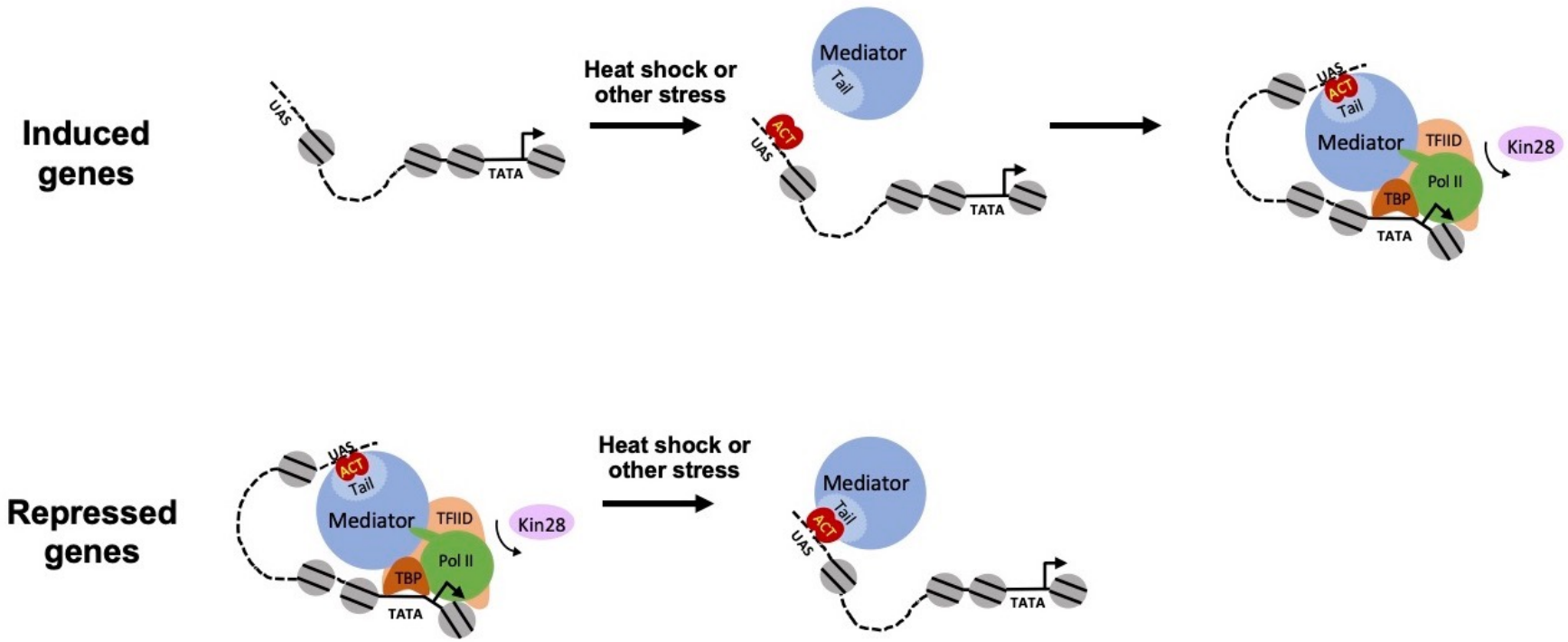

Supplemental Fig S14. Cartoon of Mediator recruitment and transcriptional activation. Under normal growth conditions (top), Mediator is recruited via its tail module by an activator bound to a UAS, and in turn recruits components of the PIC, with TBP being required for Mediator transit from UAS to the proximal promoter, which may or may not possess a consensus TATA element. Association of Mediator with the proximal promoter is normally transient, being rapidly lost upon Kin28-dependent promoter escape by Pol II, but is stabilized by depletion or inactivation of Kin28. Heat shock or other stress (such as $CdCl_2$ exposure) prevents PIC assembly and transit of Mediator to the proximal promoter of repressed genes through an unknown mechanism.

Supplemental Fig S15. Spearman correlation coefficients for 15 ChIP-seq experiments examining occupancy of Med15. Correlation coefficients were determined for reads mapping to the region 300 bp upstream of the ORF for the 300 promoters most highly occupied by Pol II after 15 min of heat shock. ”Parent” refers to YFR1321, the parent strain for the *kin28AA* strain, both of which were treated with rapamycin (see Methods). HS indicates 15 min of heat shock; samples not labeled “HS” were not subject to heat shock.

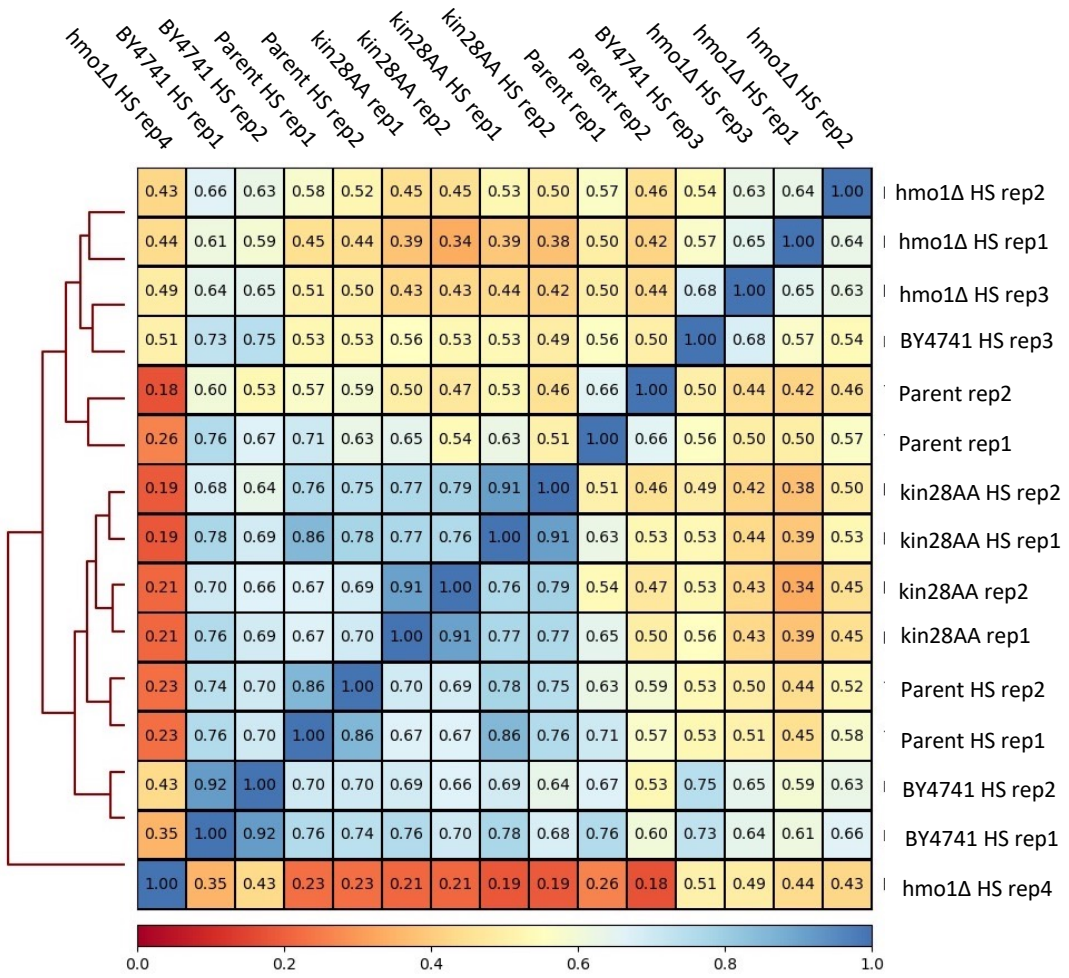

References for supplemental figures

Jeronimo, C., Langelier, M.F., Bataille, A.R., Pascal, J.M., Pugh, B.F., and Robert, F. (2016). Tail and Kinase Modules Differently Regulate Core Mediator Recruitment and Function In Vivo. Mol Cell *64*, 455-466.

Knight, B., Kubik, S., Ghosh, B., Bruzzone, M.J., Geertz, M., Martin, V., Denervaud, N., Jacquet, P., Ozkan, B., Rougemont, J.*, et al.* (2014). Two distinct promoter architectures centered on dynamic nucleosomes control ribosomal protein gene transcription. Genes Dev *28*, 1695-1709.

Morris, R.T., O'Connor, T.R., and Wyrick, J.J. (2010). Ceres: software for the integrated analysis of transcription factor binding sites and nucleosome positions in S. cerevisiae. Bioinformatics.